METHODOLOGICAL ASPECTS OF DIFFUSION ANALYSIS BY MICROSCOPY TECHNIQUES

by

Nicolas Destainville

Abstract. — Microscopy techniques play a key role in the elucidation of the dynamical organization of biophysical and biological systems. However, they provide a large amount of information, from which it can be delicate to extract the relevant one, all the more that live systems present a large variability and statistical samples are generally poor, because experiments are time-consuming. I propose here three tools that have been recently developed in this spirit. They enable one to extract such reliable information and to characterize diffusion at the surface of live cells studied by two techniques: Single Particle or Single Molecule Tracking (SPT or SMT) and Fluorescence Correlation Spectroscopy (FCS).

This note is organized as follows: a rapid survey is followed by a detailed "Methods" section.

1. Survey

1.1. Single Particle or Single Molecule Tracking: Quantification and correction of systematic errors due to detector time-averaging [1]. — When extracting the Mean Square Displacement (MSD; see Methods for the definition) from SPT or SMT trajectories, one often remarks that it displays two regimes: a short-term one with a rapid, "microscopic" diffusion coefficient D_μ and a longer-term one with a slower, "macroscopic" diffusion coefficient D_M (see Fig. 1). Such a MSD is in general very well fitted by a simple law of the form:

$$MSD(t) = \frac{L^2}{3}\left(1 - \exp(-t/\tau)\right) + 4D_M t. \tag{1}$$

The length L is interpreted as the diameter of short-term confining domains, and τ is the so-called "equilibration" or "relaxation" time. It is the typical time that the diffusing particle needs to explore its confining domain of diameter L. In other words, for $t < \tau$, the diffusion is rapid and confined. For $t > \tau$, it is slow and free. It is related to L and D_μ by $L^2 = 12 D_\mu \tau$ [**1**]. The short-term confinement can originate from several mechanisms, such as lipidic micro-domains (the so-called "rafts"), protein assemblies caused by protein-protein interactions

(see e.g. [**2**]), or hindrance by fixed linear obstacles such as the cortical actin filaments of the cytoskeleton [**3**] ("fence-and-picket" or "barrier" model). In the latter case, occasional jumps over the obstacles lead to slow long-term diffusion.

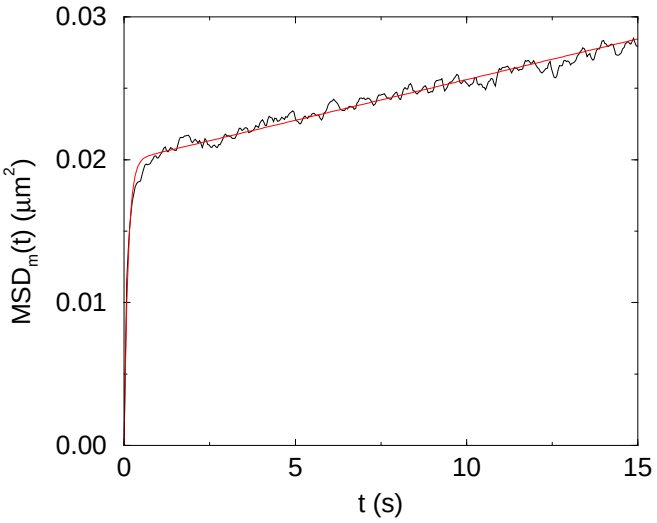

FIGURE 1. Example of experimental MSD for a μ-opioid receptor as studied in Ref. [**2**] (black), together with its fit by Eq. (1). One distinguishes the two regimes, typical of a confined, rapid diffusion at short times, followed by a slower free diffusion at larger times.

Now SPT or SMT developments rely upon a correct estimation of domain sizes and diffusion coefficients (see e.g. next section). To this respect, a common pitfall comes from the detector time-averaging effect in the case of confined diffusion at short times. Indeed, if T is the detector acquisition time, this effect cannot be neglected whenever $T > \tau/3$, because it leads to a potentially dramatic underestimation of L and D_μ. If τ_m, L_m, and $D_{\mu,m} = L_m^2/(12\tau_m)$ are the measured quantities obtained by fitting the experimental MSD by Eq. (1), then some simple mathematical formulas enable one to recover the real τ, L and D_μ from the measured ones [**1**]:

$$\tau = \tau_m - T/3, \tag{2}$$

$$L = L_m \left[2\left(\frac{\tau}{T}\right) - 2\left(\frac{\tau}{T}\right)^2 \left(1 - \exp\left(-\frac{T}{\tau}\right)\right)\right]^{-1/2}, \tag{3}$$

and

$$D_\mu = \frac{L^2}{12\tau}. \tag{4}$$

How to use these formulas is detailed in the Methods section.

1.2. Single Particle or Single Molecule Tracking: Detection of confinement and jumps in trajectories [2]. — Here we present a tool [**2**] which enables the detection of confinement, whether temporary or permanent, by any kind of micro-domain: cytoskeleton meshwork, lipid domains or protein assemblies. In addition, it is able to detect a local loss of confinement due to jumps above linear obstacles in SPT or SMT trajectories (see 1.3). If the observed diffusional behavior is suspected to be described by a fence-and-picket model, this tool is useful to quantify the number of observed jumps and to decide whether it is sufficiently important to explain the measured long-term diffusion coefficient. Indeed, if $\tau_{\rm conf}$ is the average confinement time into domains, that is to say the average time between two successive jumps, then the relation $L^2 = 4D_M\tau_{\rm conf}$ provides the value of $\tau_{\rm conf}$, after measuring L and D_M (and possibly correcting L: see 1.1) . The expected number of jumps is then given by $N_{\rm jumps}^{\rm expected} = T_{\rm traj}/\tau_{\rm conf}$, where $T_{\rm traj}$ is the time length of the trajectory.

Refining a former algorithm by R. Simson et al. [**4**], Meilhac et al. have proposed an algorithm that was proven to be more reliable in this context to detect jumps [**2**]. Its main interest is that even if, because of statistical noise, it can only detect a finite fraction of jumps – typically 50 to 70 % –, it makes very little false detection. Therefore the real number of jumps $N_{\rm jumps}^{\rm real}$ can be estimated by the detected one multiplied by a numerical factor, of order 1 to 2. This factor must be specifically calculated for the given problem under consideration, with the help of numerical simulations, because it depends on the typical values of L^2, D_M and D_μ. The so-obtained $N_{\rm jumps}^{\rm real}$ can then be compared to what is expected in a barrier model, $N_{\rm jumps}^{\rm expected}$. The algorithm is detailed in the Methods section below.

1.3. Fluorescence Correlation Spectroscopy at variable observation area and diffusion on a semi-permeable meshgrid [5, 6, 7]. — This tool concerns again diffusion on an actin-like meshgrid. But in this case, the observation technique is not an invidual-object one, but an ensemble one, the FCS. This is a powerful and common tool used to measure an average long-term diffusion coefficient, D_M. It is based upon an analysis of the fluorescence fluctuations in a small volume or membrane area [**8, 9**]. Recently, it has been demonstrated that using an observation domain of variable diameter, FCS is able to discriminate between different modes of diffusion at the surface of cells, in particular between free diffusion, diffusion in raft-like or protein assemblies and, again, diffusion on a semi-permeable meshgrid. We suppose that the observation illumination profile is Gaussian with waist w. Once determined (see Methods), the correlation function can be (more or less) fitted by the law:

$$C(t) = \frac{1}{1 + t/t_{1/2}}. \tag{5}$$

In this expression, $t_{1/2}$ is the time at which the FCS correlation function gets reduced by a factor 2. Instead of fitting by Eq. (5), this latter definition of $t_{1/2}$ must be preferred in the present context. It can be measured with a good precision. Then if w is the waist of the observation profile, it can be proven that

$$t_{1/2} \simeq \frac{1}{4D_M}(w^2 - (Const.L)^2), \tag{6}$$

where L is the mesh size and the constant will be discussed in the Methods section. Experimentally, the measure of $t_{1/2}$ at several waists enables one to infer: (i) the value of D_M; (ii) the value of L, the mesh-size, of biological interest. This is the core of FCS at variable observation area [**5, 6, 7**].

2. Methods

2.1. Single Particle (or Molecule) Tracking. — We denote by $\mathbf{X}(t_i)$ the two-dimensional successive positions of the particle at discrete observation times $t_0, t_1, \ldots, t_N$ separated by δt: $t_i = i\delta t$. At standard video rate, $\delta t = 40$ ms (33 ms in the US or in Japan). The MSD at time $t = S\delta t$ is calculated by

$$MSD(t) = \frac{1}{N-S+1}\sum_{i=0}^{N-S}[\mathbf{X}(t_i) - \mathbf{X}(t_{i+S})]^2. \tag{7}$$

It is the average of the squared displacement during a time interval of duration s. If some points are lacking in the trajectory because their acquisition failed, the corresponding squares are omitted in the sum and the normalization prefactor must be adapted consequently.

The time s must be chosen to vary between 0 (and $MSD(0) = 0$) and $s_{\max}$ such that $\tau \ll s_{\max} \ll t_N$. The first condition ensures that the cross-over at τ will effectively be seen. The second one is required to avoid excessive statistical noise. Typically, one needs $s_{\max}/\tau > 5$ and $t_N/s_{\max} > 20$. Once $MSD(s)$ is plotted, it must be fitted by Eq. (1). The measured parameters are denoted by τ_m, L_m, and D_M. The latter value can be kept as such because it cannot be affected by averaging effects. As for $D_{\mu,m}$, it is given by $D_{\mu,m} = L_m^2/(12\tau_m)$ [**1**].

2.2. Correcting detector averaging effects [**1**]**.** — We denote by T the detector acquisition time. Note that T need not being equal to δt. Of course, $T \leq \delta t$.

If the measured equilibration time, τ_m, is shorter than $3T$, then the measured values must be corrected. In addition, if $\tau_m < 2T/3$, then the measured "microscopic" parameters τ_m and $D_{\mu,m}$ must be considered as irrelevant and the acquisition time T must be considered as too high for the experimental system under consideration. If $2T/3 \leq \tau \leq 3T$, then Eqs. (2-4) must be used to obtain the real values of τ, L, and D_μ.

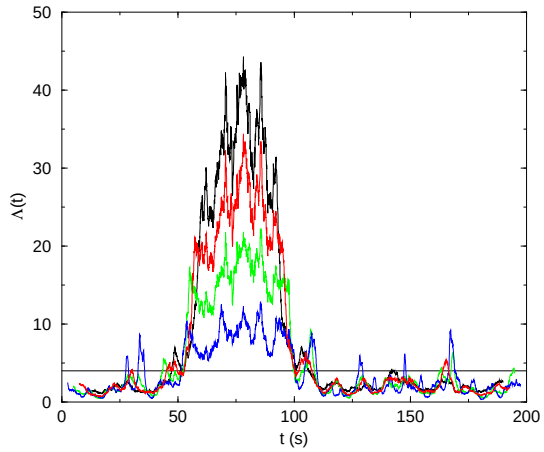

FIGURE 2. Example of profile $\Lambda(t)$ for a simulated trajectory of duration 200 s. The diffusion is free (pure Brownian) with diffusion coefficient $D_\mu = 0.06\ \mu\text{m}^2\text{s}^{-1}$, except on the time interval [50,100], where it is confined in a rectangular box of sides 400 nm × 560 nm. Four profiles are plotted for $\Delta t = 5, 10, 15$ and 20 s, from bottom to top. The higher Δt, the better the signal: the profile is generally below the threshold value $\Lambda = 4$ for a Brownian trajectory (horizontal line), and neatly above this value for confined diffusion.

2.3. Detecting confinement [2]. — The variance of the trajectory on a time interval $[t, t+\Delta t]$ with $\Delta t = n\delta t$ is defined by

$$\Delta X^2(t,\Delta t) = \frac{1}{n+1}\sum_{i=0}^{n}\mathbf{X}^2(t_i) - \left[\frac{1}{n+1}\sum_{i=0}^{n}\mathbf{X}(t_i)\right]^2. \tag{8}$$

For a pure Brownian motion, this variance is proportional to $D_\mu\Delta t$. The idea of the algorithm proposed in Ref. [**2**] is to detect a deviation to this ideal case: if the trajectory is confined on the interval, then ΔX^2 will be smaller than this expected value. Thus we define the confinement index Λ as follows

$$\Lambda(t) = \frac{D_\mu\Delta t}{\Delta X^2(t,\Delta t)}. \tag{9}$$

One demonstrates that $\Lambda_{\text{Brown}} \leq 4$ with a good probability for a pure Brownian trajectory, independently of δt and D. By contrast, if one considers confined diffusion in a square box of side L, one gets $\Delta X^2 = L^2/6$, and

$$\Lambda_{\text{conf}} = 6D_\mu\Delta t/L^2. \tag{10}$$

Confinement (permanent or temporary) will be distinguishable from pure Brownian trajectories if $\Lambda_{\text{conf}} \gg \Lambda_{\text{Brown}}$ *i.e.* if $\Lambda_{\text{conf}} \gg 4$ or $D_\mu\Delta t/L^2 \gg 2/3$. Note that Δt must be sufficiently large to enable detection of confinement. A commented example is provided in Fig. 2.

In practice, the calculation of Λ requires both the value of $\Delta X^2(t, \Delta t)$ for each interval $[t, t + \Delta t]$, as explained above, and the value of D_μ. Since this value can vary significantly along a same trajectory [**2**], a local value, $D_\mu(t)$, is needed. It must be calculated on an interval $[t, t + n'\delta t]$, with $n' \sim 100$ to avoid excessive statistical noise. This calculation relies on a calculation similar to the one given in Eq. (7), by fitting only the first 2 or 3 points to get D_μ (only), because $MSD(t) \simeq 4D_\mu t$ at short times.

The examination of $\Lambda(t)$ indicates if the trajectory is either free, or confined on all the trajectory, or only on a fraction of it (Transient Confinement Zones or TCZ). If one chooses several increasing values of Δt, free-diffusion periods will display a constant Λ below the threshold value of 4, whereas transient confinement will lead to increasing values of Λ (see Fig. 2).

2.4. Detecting jumps [2]. — The detection of jumps is based on the same confinement index Λ. The idea here is to exploit the following observation: when the trajectory is devoid of jumps on the interval $[t, t+n'\delta t]$, $\Lambda(t)$ has a high value as discussed above, because $\mathbf{X}(t)$ is confined in a single domain. Now, if there are one or several jumps in this interval, the trajectory visits successively several domains in $[t, t+n'\delta t]$. In other words, the tracked particle is virtually in a twice (or more) larger domain. Thus $\Delta X^2(t, \Delta t)$ is significantly higher than in the previous case, and $\Lambda(t)$ is smaller. In addition, the fact that D_μ can vary along the trajectory must also been taken into account.

In practice, the profile $\Lambda(t)$ is calculated as explained above. Jumps are then characterized by gaps in the profile, as exemplified in Fig. 3. It can be demonstrated that these gaps have a minimum value

$$\Lambda_{\text{jump}} = 2\Lambda_{\text{conf}}/5. \tag{11}$$

To distinguish gaps from random fluctuations of Λ, they must also have a certain duration. It is demonstrated in Ref. [**2**] that the best compromise is to characterize gaps by $\Lambda(t) > \alpha\overline{\Lambda}$ on a time interval longer than $\Delta t/2$. Here $\overline{\Lambda}$ is the average value of Λ on the whole trajectory, and $\alpha = 0.7$. Moreover, the efficiency of the detection relies on a neat separation between short-term and long-term diffusion: the condition

$$D_\mu > 20\ D_M \tag{12}$$

must be satisfied. The choice of Δt is also crucial: it must be as large as possible to enhance the signal, but also as small as possible to separate at best close jumps; $\Delta t = \tau_{\text{conf}}/3$ is also a good compromise, where we recall that $\tau_{\text{conf}} = L^2/(4D_M)$. Finally, since D_μ can vary along the trajectory, it is recommended to truncate the trajectory in ~ 30 s segments where jumps are detected independently (see the figure).

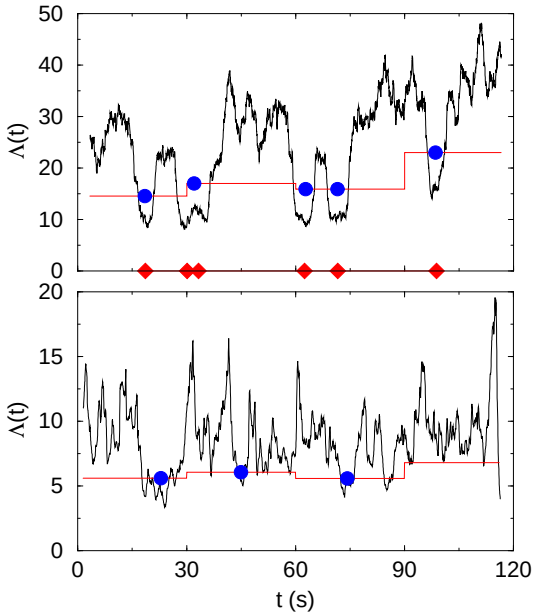

FIGURE 3. Top: Profile $\Lambda(t)$ for a numerical trajectory with $\tau_{res} = 20$ s. We have also plotted in red the threshold $\alpha\overline{\Lambda}$ with $\alpha = 0.7$, calculated on 30 s segments. Real jumps have been directly detected in the trajectory simulation and are represented by diamonds, whereas the ones detected by the algorithm are signaled by circles. Five jumps have been detected, among which one double jump (detected only once because the two jumps are too close). Bottom: Profile for an experimental trajectory (from Ref. [**2**]), with three detected jumps. Some intervals where $\Lambda(t)$ is below the threshold are not considered as jumps because they are not long enough.

3. Fluorescence correlation spectroscopy

Now we quit the domain of single particle techniques and we turn to FCS, which provides ensemble information. In FCS experiments, the two-time autocorrelation function, $g^{(2)}(t)$, indicates the average degree of correlation between measures of the number of photons, $n(s)$ and $n(s+t)$ collected by the detector, at different times s and $s+t$ [**8, 9**]. Again, the observation time is discrete: $t_i = i\delta t$, $i = 0, \ldots, N$. Each measure $n(t_i)$ is a number of photons detected per sampling time δt. More precisely, the correlation function is defined as follows:

$$g^{(2)}(t) = \frac{\langle n(t')n(t'+t)\rangle}{\langle n(t')\rangle^2}. \tag{13}$$

In this definition, if $t = S\delta t$ then

$$\langle n(t')n(t'+t)\rangle \equiv \frac{1}{N-S+1}\sum_{i=0}^{N-S} n(t_i)n(t_{i+S}) \tag{14}$$

and

$$\langle n(t') \rangle \equiv \frac{1}{N+1} \sum_{i=0}^{N} n(t_i). \tag{15}$$

Then it is demonstrated [**9**] that $g^{(2)}(t)$ has the typical form:

$$g^{(2)}(t) = 1 + \frac{1}{\langle \rho \rangle S_{\text{eff}}} C(t), \tag{16}$$

where: (i) $\langle \rho \rangle$ is the average density of fluorophores in the system; (ii) $S_{\text{eff}} = \pi w^2$ is the effective observation surface of the Gaussian illumination source of waist w; (iii) $C(t)$ is a reduced correlation function such that $C(t = 0) = 1$ and $C(t = \infty) = 0$. Then the so-called decorrelation time, $t_{1/2}$, is defined by

$$C(t_{1/2}) = \frac{1}{2}. \tag{17}$$

The typical behavior of $t_{1/2}$ for diffusion on a meshgrid of semi-permeable barriers is displayed in Fig. 4. By contrast to free diffusion, $t_{1/2}(w^2)$ vanishes for a non-zero value of w^2, denoted by $w_c^2 \simeq 0.362 L^2$, with L the mesh size. This fact has been demonstrated by numerical arguments [**5, 6**] before being proved rigorously [**7**].

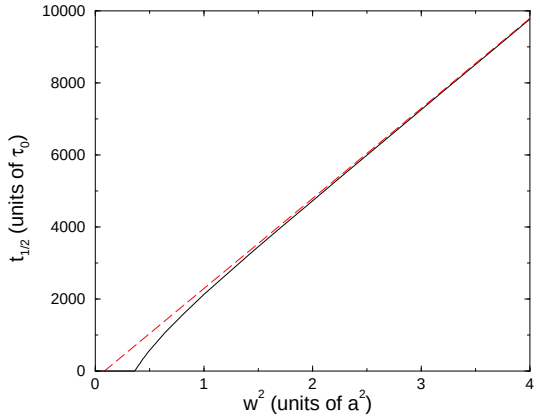

FIGURE 4. Plot of the decorrelation time, $t_{1/2}$, in arbitrary unit τ_0, as a function of the observation domain area, w^2, in the case of a Gaussian illumination profile of waist w. $D_M = 10^{-4} L^2 \tau_0^{-1}$ is also written in terms of arbitrary units. The continuous line shows the numerical solution of $C(t_{1/2}) = 1/2$ [**7**]. The dotted line is the result of the affine asymptotic expansion of $t_{1/2}$, valid at large w [**7**]. It meets the w^2 axis at $w^2 = 1/12 \simeq 0.0833$. The numerical solution meets the same axis at $w_c^2 \simeq 0.362$.

If one can only access experimentally large values of w^2 as compared to w_c^2, the behavior of $t_{1/2}$ becomes affine, as shown in the figure. The intersection with the w^2 axis is still positive, but with a smaller value, $w^2 = 1/12$ [**7**]. Therefore,

as discussed in detail in this reference, the choice of the value of the constant in Eq. (6) depends on the range of accessible waists. Note also that in the case of particle transiently trapped in raft-like domains, it has been shown that the intercept of $t_{1/2}$ with the time axis becomes positive, whereas it was negative in the previous case. Thus this technique enables one to distinguish between different diffusion modes [**5, 6**].

Before closing this section, we should also mention that the fluorophore choice is critical in this context: its intrinsic fluorescence fluctuations must have a short characteristic time, shorter than a few micro-seconds (see the discussion in Ref. [**7**]).

References

[1] N. Destainville, L. Salomé, Quantification and correction of systematic errors due to detector time-averaging in single molecule tracking experiments, *Biophys. J.* **90**, L17-L19 (2006).

[2] N. Meilhac, L. Le Guyader, L. Salomé, N. Destainville, Detection of confinement and jumps in single protein membrane trajectories, *Phys. Rev. E* **73**, 011915 (2006).

[3] K. Suzuki, K. Ritchie, E. Kajikawa, T. Fujiwara, and A. Kusumi, Rapid Hop Diffusion of a G-Protein-Coupled Receptor in the Plasma Membrane as Revealed by Single-Molecule Techniques, *Biophys. J.* **88**, 3659-3680 (2005).

[4] R. Simson, E.D. Sheets, and K. Jacobson, Detection of temporary lateral confinement of membrane proteins using single-particle tracking analysis. *Biophys. J.* **69**, 989-993 (1995).

[5] L. Wawrezinieck, H. Rigneault, D. Marguet, and P.-F. Lenne, Fluorescence Correlation Spectroscopy Diffusion Laws to Probe the Submicron Cell Membrane Organization, *Biophys. J.* **89**, 4029-4042 (2005).

[6] J. Wenger, F. Conchonaud, J. Dintinger, L. Wawrezinieck, T.W. Ebbesen, H. Rigneault, D. Marguet, and P.-F. Lenne, Diffusion Analysis within Single Nanometric Apertures Reveals the Ultrafine Cell Membrane Organization, *Biophys. J.* **92**, 913-919 (2007).

[7] N. Destainville, Theory of fluorescence correlation spectroscopy at variable observation area for two-dimensional diffusion on a meshgrid, *Soft Matter* (in press, 2008; preprint available at `http://arxiv.org/abs/0711.4699`).

[8] D. Magde, E. Elson, and W.W. Webb, Thermodynamic Fluctuations in a Reacting System – Measurement by Fluorescence Correlation Spectroscopy, *Phys. Rev. Lett.* **29**, 705-708 (1972).

[9] R. Rigler, and E.S. Elson (Eds.), Fluorescence Correlation Spectroscopy: Theory and Applications, Springer, New York, 2001.

Nicolas Destainville, , Laboratoire de physique théorique, CNRS/Université Toulouse 3, 118 route de Narbonne, 31062 Toulouse Cedex; Institut de Pharmacologie et Biologie Structurale, CNRS/Université Toulouse 3, 205 route de Narbonne, 31077 Toulouse Cedex.
E-mail : nicolas.destainville@irsamc.ups-tlse.fr